Beryllium-9 NMR Study of Solid Bis(2,4-pentanedionato-*O,O′*)beryllium and Theoretical Studies of ^{9}Be Electric Field Gradient and Chemical Shielding Tensors. First Evidence for Anisotropic Beryllium Shielding

David L. Bryce and Roderick E. Wasylishen*

Department of Chemistry, Dalhousie University, Halifax, Nova Scotia, Canada, B3H 4J3

Received: June 3, 1999

Despite the favorable NMR properties of ^{9}Be ($I = {}^{3}/_{2}$), NMR spectroscopy of this nucleus in the solid state remains comparatively unexplored, perhaps owing to the extreme toxicity of beryllium and its compounds. We present here an integrated experimental and theoretical study of the Be chemical shielding (CS) and electric field gradient (EFG) tensors in bis(2,4-pentanedionato-*O,O′*)beryllium [Be(acac)$_2$]. Interpretation of the ^{9}Be NMR data was facilitated by crystal X-ray diffraction results, which indicate two crystallographically unique sites (Onuma, S.; Shibata, S. *Acta Crystallogr.* **1985**, *C41*, 1181). Beryllium-9 NMR spectra acquired at 4.7 and 9.4 T for magic-angle spinning (MAS) and stationary samples have been fitted in order to extract the nuclear quadrupole coupling constant (C_Q), asymmetry parameter (η), and isotropic chemical shift (δ_{iso}). The best-fit nuclear quadrupole parameters for the two sites were determined to be $C_Q(1) = -294 \pm 4$ kHz, $\eta(1) = 0.11 \pm 0.04$; $C_Q(2) = -300 \pm 4$ kHz, $\eta(2) = 0.15 \pm 0.02$. Our analyses of the stationary samples also reveal a definite anisotropy in the beryllium CS tensor and allow us to place upper and lower limits on the spans of 7 and 3 ppm. This is the first evidence for anisotropic shielding in beryllium. Ab initio calculations of the beryllium CS tensors in Be(acac)$_2$ at the RHF level indicate spans ranging from 7 to 9 ppm; this represents a substantial fraction of the total known chemical shift range for Be (<50 ppm). The calculated C_Qs are also in good agreement with the experimental results. To put the Be(acac)$_2$ results in context, calculations of the beryllium CS tensors for a series of compounds encompassing the known range of ^{9}Be chemical shifts are also presented. The calculations are in outstanding accord with experimental data from the literature. On the basis of calculations for linear molecules, it is shown that the assumption that the ^{9}Be chemical shift is governed essentially by the diamagnetic term is erroneous. For some of these molecules, the calculated Be CS tensor spans are greater than the total known chemical shift range.

Introduction

Most NMR-active isotopes possess quadrupolar nuclei ($I > {}^{1}/_{2}$).[1,2] In the solid state, the observation of the spectra of half-integer spin quadrupolar nuclei is a rapidly growing area of research partly as a result of the potential applications to the materials and biological sciences, where quadrupolar nuclei such as ^{27}Al, ^{17}O, ^{11}B, and ^{23}Na, for example, are of interest.[3,4] Recent advances in experimental solid-state NMR methodology for half-integer spin quadrupolar nuclei have been summarized by Smith and van Eck.[5] An important advantage of using NMR to study solids is its ability to characterize not only the isotropic values of the various NMR interactions but also the individual tensor components, which, in principle, should provide more insight into the nature of the interaction as well as the local molecular and electronic structures. Over the past decade, improved computational methods and access to more powerful computers have made practical the reliable calculation of NMR interaction tensors, consequently making such calculations extremely valuable to the solid-state NMR spectroscopist for the interpretation of experimental data.[6,7] The recent review of Helgaker et al.[8] provides an overview of ab initio methods for the calculation of NMR shielding and indirect spin−spin coupling constants.

Beryllium-9 ($I = {}^{3}/_{2}$) NMR in the solid state remains relatively unexplored, especially for small molecules for which ab initio calculations of the electric field gradient (EFG) and chemical shielding (CS) tensors are feasible. This is despite its relatively small quadrupole moment ($Q = 5.288 \times 10^{-30}$ m^2),[9] receptivity relative to ^{13}C of 78.7, and 100% natural abundance. The lack of activity in this area of NMR research is likely in part due to the extreme toxicity of this element;[10] however, the narrow chemical shift range (<50 ppm) may also detract from its utility as a characterization tool. Summaries of representative known isotropic chemical shifts for ^{9}Be-containing compounds measured in solution may be found in the literature.[11] Solid-state ^{9}Be NMR has been used recently for characterizing a variety of minerals,[12] which are comparatively nontoxic;[13] however, simpler systems composed of relatively small molecules remain generally unexamined. Bis(2,4-pentanedionato-*O,O′*)beryllium [bis(acetylacetonato)beryllium(II), Be(acac)$_2$] was first examined in solution using ^{9}Be NMR by Wehrli[14] and more recently by Kanakubo et al.[15] Unfortunately, the dual-spin probe relaxation method employed in these solution studies can only provide $[C_Q^2(1 + \eta^2/3)]^{1/2}$, where C_Q is the nuclear quadrupole coupling constant and η is the asymmetry parameter. In addition, solution studies provide no information on CS tensors. One of the main advantages of studying quadrupolar nuclei in the solid state rather than in solution is that C_Q and η may both be determined; furthermore, the CS tensor can be characterized. Acetylacetonato

* To whom correspondence should be addressed. Phone: 902-494-2564. Fax: 902-494-1310. Email:rodw@is.dal.ca.

10.1021/jp9918003 CCC: $18.00
Published on Web 08/20/1999

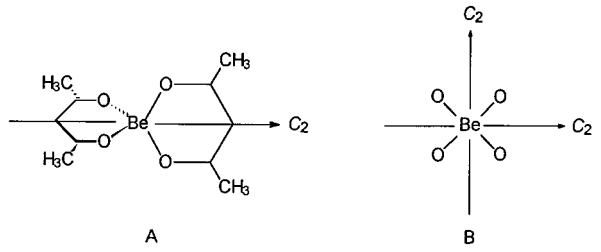

Figure 1. $Be(acac)_2$ molecule. The four oxygen atoms are coordinated in an approximately tetrahedral arrangement about the central Be atom. An isolated molecule has perfect D_{2d} symmetry; the unique C_2 rotation axis is indicated in part A. Shown in part B is a view along the unique axis; the two remaining C_2 axes are indicated in this projection.

complexes of cobalt,[16−18] aluminum,[19−21] calcium and magnesium,[22] and gallium and indium[21] have been studied previously via NMR. Such complexes are appealing owing to the inherent high degree of symmetry at the metal center; this symmetry ensures that the quadrupolar coupling constant is not impractically large. For complexes that have been studied both in solution and in the solid state, and in different solvents, there are often significant discrepancies in the reported C_Q values, implying a strong dependence of C_Q on the nature of the solvation shell.

We present here a ^{9}Be NMR study of $Be(acac)_2$ in the solid state. Its structure (Figure 1) has been previously determined both in the gas phase by electron diffraction[23] and in the solid state by X-ray diffraction[24] (monoclinic, $\beta = 100.79°$, space group $P2_1$). The molecules have approximately the expected D_{2d} symmetry in the gas phase, while two crystallographically distinct, slightly distorted molecules are present in the solid state. Analyses of the ^{9}Be NMR spectra of stationary and magic-angle-spinning (MAS) powder samples of $Be(acac)_2$ obtained at two different applied magnetic fields were carried out in order to determine the nuclear quadrupolar parameters for each of the two distinct beryllium sites. It has been stated in the literature that the shielding range of ^{9}Be is no greater than that of hydrogen.[25] Although numerous ^{1}H shielding tensors have been characterized,[26] to date no experimental characterization of a ^{9}Be shielding tensor has been reported.

In addition to the experimental determination of the ^{9}Be EFG and CS tensors in $Be(acac)_2$, we propose orientations for these tensors in the molecular frame based both on perfect D_{2d} symmetry and on ab initio calculations employing atomic coordinates from crystal X-ray diffraction or electron diffraction data. Calculations of the CS tensors for a range of beryllium-containing molecules including $Be(acac)_2$, $Be(H_2O)_4^{2+}$, C_5H_5BeX (X = Cl, CH_3, BH_4), and representative two-coordinate and three-coordinate complexes provide some insight into the factors affecting the observed isotropic chemical shifts for these molecules. From our data, it is evident that the beryllium chemical shift is not governed by the diamagnetic contribution, as had been previously assumed.[27,28]

Theory and Background: Nuclear Magnetic Shielding and Quadrupolar Interactions

The Hamiltonian operator for the beryllium nucleus in $Be(acac)_2$ may be written as

$$\hat{H} = \hat{H}_Z + \hat{H}_{CS} + \hat{H}_Q \quad (1)$$

where the Zeeman (Z), chemical shielding (CS), and quadrupolar (Q) Hamiltonians are of concern. For stationary samples, all three of these contribute to the observed spectrum. The combined Zeeman and chemical shielding Hamiltonian is simply

$$\hat{H}_{Z,CS} = -\frac{\gamma h}{2\pi}[\hat{\mathbf{I}}\cdot(\mathbf{1} - \sigma)\cdot B_0] \quad (2)$$

where B_0 is the external applied magnetic field, γ is the magnetogyric ratio of the nucleus, $\hat{\mathbf{I}}$ is the nuclear spin angular momentum operator, **1** is the unit tensor, and σ is the nuclear magnetic shielding tensor. For a powder sample, the component of the shielding tensor along B_0 (the space-fixed Z axis) may be written as

$$\sigma_{ZZ} = \sigma_{11}\sin^2\theta\cos^2\phi + \sigma_{22}\sin^2\theta\sin^2\phi + \sigma_{33}\cos^2\theta \quad (3)$$

where σ_{11}, σ_{22}, and σ_{33} are the principal components of σ, θ is the angle between σ_{33} and B_0, and ϕ is the angle between σ_{11} and the projection of B_0 onto the plane defined by σ_{11} and σ_{22}. The isotropic component of the nuclear magnetic shielding tensor, $\sigma_{iso} = (\sigma_{11} + \sigma_{22} + \sigma_{33})/3$, is directly related to the isotropic chemical shift by the following equation:

$$\delta_{iso,sample} = \frac{\sigma_{iso,ref} - \sigma_{iso,sample}}{1 - \sigma_{iso,ref}} \times 10^6 \quad (4)$$

This is simplified when $\sigma_{iso,ref} \ll 1$ to give

$$\delta_{iso,sample} \cong \sigma_{iso,ref} - \sigma_{iso,sample} \quad (5)$$

as is the case for beryllium. Since there is no established absolute shielding scale for ^{9}Be, we will refer to the chemical shift tensor and δ_{iso} when discussing experimental results, while the chemical shielding tensor is discussed in conjunction with the results of the ab initio calculations. Of course, the orientations of the shift and shielding tensors are identical. The *span* (Ω) of the chemical shielding or shift tensor is defined as[29]

$$\Omega = \sigma_{33} - \sigma_{11} = \delta_{11} - \delta_{33} \quad (6)$$

In the high-field approximation (i.e., when the Zeeman splittings are much larger than the quadrupolar splittings), the quadrupolar Hamiltonian is given to first order by

$$\hat{H}_Q = h\frac{C_Q}{8I(2I-1)}(3\hat{I}_z^2 - \hat{\mathbf{I}}^2)(3\cos^2\theta - 1 + \eta\sin^2\theta\cos 2\phi) \quad (7)$$

The angles θ and φ define the orientation of B_0 in the EFG tensor principal axis system in a manner analogous to that described for the chemical shielding tensor. The components of the EFG tensor in its principal axis system are defined such that

$$|V_{ZZ}| \geq |V_{YY}| \geq |V_{XX}| \quad (8)$$

and the quadrupolar coupling constant is defined as

$$C_Q = \frac{eQV_{ZZ}}{h} \quad (9)$$

The asymmetry parameter, η, is defined as

$$\eta = \frac{V_{XX} - V_{YY}}{V_{ZZ}} \quad (10)$$

Under conditions of rapid MAS, both the chemical shielding and first-order quadrupolar interactions are averaged to their isotropic values. Consequently, when spectra of MAS samples are analyzed, only the Zeeman and second-order quadrupolar

interactions need to be considered, in addition to δ_{iso}. Expressions for the second-order quadrupolar Hamiltonian may be found in the original literature or in review articles.[2,5,30] In general, there are cases where perturbation theory does not apply, e.g., when $\hat{H}_Q \cong \hat{H}_Z$.

Samoson has given general equations that describe how the apparent isotropic chemical shift is modified by the second-order quadrupolar interaction under conditions of MAS.[31] For a spin $^3/_2$ nucleus, the center of gravity of the observed central transition centerband is displaced from the true isotropic resonance frequency by

$$\Delta\nu_{+1/2,-1/2} = -\frac{1}{40}\left(\frac{C_Q^2}{\nu_L}\right)\left(1+\frac{\eta^2}{3}\right) \qquad (11)$$

Furthermore, the position of the $\pm^3/_2 \leftrightarrow \pm^1/_2$ satellite transition centerbands with respect to the central transition centerband is given by[31]

$$\Delta\nu_{\pm3/2,\pm1/2} - \Delta\nu_{+1/2,-1/2} = \frac{3}{40}\left(\frac{C_Q^2}{\nu_L}\right)\left(1+\frac{\eta^2}{3}\right) \qquad (12)$$

Thus, under appropriate conditions, the satellite transition centerbands should be resolved from the central transition centerband.

Experimental

***Caution**: Beryllium and its compounds are **extremely toxic** and should be handled with care.*[10] Bis(acetylacetonato)-beryllium(II) (Strem Chemical) was recrystallized from benzene before being ground into a fine powder and packed into 7.5 and 4.0 mm (o.d.) zirconium oxide rotors. All spectra were acquired on Varian/Chemagnetics CMX Infinity ($B_0 = 4.7$ T, $\nu_L = 28.1$ MHz) and Bruker AMX ($B_0 = 9.4$ T, $\nu_L = 56.2$ MHz) spectrometers, with high-power proton decoupling. Referencing and setup for the ^{9}Be nucleus were carried out using 0.1 M $BeSO_4$ (aq) [$\delta_{iso}(Be(H_2O)_4^{2+}) = 0.00$ ppm], for which 90° pulses of 3.8 μs (AMX) and 4.6 μs (CMX) were used. Solid 90° pulses employed for $Be(acac)_2$ were between 0.6 and 1.0 μs. Recycle delays varied between 30 and 60 s. Spectra of stationary and MAS samples are the result of the addition of 1536 and 1024 scans, respectively, followed by Fourier transformation. Acquisition times of 100−120 ms were used. Cross polarization (CP) was not employed because of the observed pronounced distortion of the central transition line shape caused by this technique. Barrie has reported similar problems in the ^{27}Al NMR spectra of $Al(acac)_3$.[20] MAS samples were spun at a rate of 5.0 kHz to suppress the first-order quadrupolar interaction and chemical shielding anisotropy. Spectra were analyzed using the WSOLIDS1 software package, which was developed in this laboratory.[32] This package incorporates the space-tiling algorithm of Alderman et al. for the efficient generation of powder patterns.[33] Ab initio calculations (RHF) of CS and EFG tensors were carried out on an IBM RISC 6000 workstation using Gaussian 94[34] and Gaussian 98.[35] Basis sets for all atoms were obtained from the Extensible Computational Chemistry Environment Basis Set Database.[36] The GIAO method[37,38] was used for calculating the CS tensors. Further details concerning the ab initio calculations are given in the following discussion.

Results and Discussion

NMR Spectroscopy. To characterize both the quadrupolar and the nuclear magnetic shielding interactions of ^{9}Be in $Be(acac)_2$, we first focused on extracting C_Q, η, and δ_{iso} from the spectra of MAS samples acquired at 4.7 and 9.4 T via simulations (Table 1). On the basis of the crystal structure, which shows two nonequivalent molecules per unit cell,[24] it was anticipated that a two-site model would be required to fit the spectra. Figure 2 shows the central transition centerband part of the experimental and simulated spectra for a MAS sample at 9.4 T. The line widths, about 65 Hz at half-height, are remarkably narrow for a quadrupolar nucleus. Shown in the insets are the calculated central transition centerband line shapes for each of the two sites. The fitting process required many iterations, and an acceptable fit is based on visual inspection. Attempts to fit the spectra are not completely based on a trial-and-error approach, however. In the present case, the magnitude of the quadrupolar coupling constant was obtained by simulations of a single site; the breadth of the resulting line shape was matched to the experimental spectrum. Additionally, an upper limit on the asymmetry parameters of 0.25 was ascertained by comparing SATRAS simulations[1,39] to a spectrum acquired experimentally. Attempts to fit the spectra based on the assumption of a single crystallographic site were fruitless. The results of the best-fit simulations (Table 1) show that both C_Q and η are identical within experimental error for the two unique sites in the crystal, but the optimum fit was achieved when the parameters were not identical for the two sites. The average

TABLE 1: Best-Fit ^{9}Be Chemical Shift[a] and Quadrupolar Parameters in $Be(acac)_2$

	site 1	site 2
C_Q/kHz	-294 ± 4	-300 ± 4
η	0.11 ± 0.04	0.15 ± 0.02
δ_{11}/ppm	1.86	2.70
δ_{22}/ppm	1.86	2.70
δ_{33}/ppm	−1.56	−3.90
Ω/ppm	3.42	6.60
$\Delta\delta = \delta_{iso}(1) - \delta_{iso}(2)$/ppm	0.22 ± 0.01	0.22 ± 0.01
α[b]/deg	0	0
β/deg	0	0
γ/deg	0	0

[a] For coincident CS and EFG tensors. [b] Euler angles describe the rotations required to bring the EFG tensor into coincidence with the CS tensor.

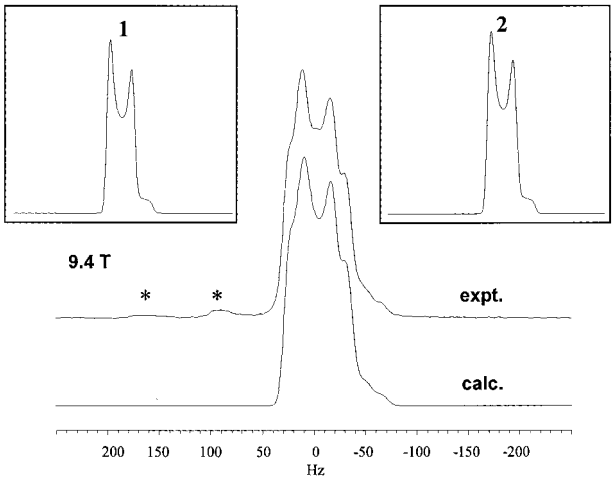

Figure 2. Experimental and calculated ^{9}Be NMR spectra of a MAS sample of solid $Be(acac)_2$,with $\nu_{rot} = 5.0$ kHz, $B_0 = 9.4$ T, and $\nu_L = 56.2$ MHz. The experimental spectrum is the sum of 1024 acquisitions. Best-fit simulation parameters are given in Table 1. The asterisks above the experimental spectrum mark the $\pm^3/_2 \leftrightarrow \pm^1/_2$ satellite transition centerbands. Shown in the insets are the simulated spectra for sites 1 and 2; the best-fit calculated spectrum is the sum of these.

value of C_Q obtained in our solid-state investigation, 298 kHz, is slightly less than the value reported for Be(acac)$_2$ in acetonitrile solution by Kanakubo et al.,[15] $C_Q = 348$ kHz. The dual-spin probe technique employed in their study can, of course, only yield $[C_Q^2(1 + \eta^2/3)]^{1/2}$; a negligible value of η is normally assumed. The success of this technique also relies on a reliable estimate of the square of the vibrationally averaged ^{1}H−^{13}C-(methine) dipolar coupling constant, in addition to several other assumptions. Quadrupolar parameters determined in the solid state have the additional advantage that the "solvent effects" are well-defined; the surrounding molecules have long-range crystallographic order. For comparison, consider Co(acac)$_3$. In the solid state, a single-crystal ^{59}Co NMR study[18] yielded the values $C_Q = 5.53 \pm 0.10$ MHz and $\eta = 0.219 \pm 0.005$. In acetonitrile solution, $C_Q = 4.8$ MHz at 298.8 K,[16] while in acetone and diglyme, $C_Q = 4.5$ MHz, and in benzene, $C_Q = 4.2$ MHz at 298 K.[16,40] For Al(acac)$_3$, ^{27}Al NMR studies in the solid state[19] revealed values of $C_Q = 3.03 \pm 0.01$ MHz and $\eta = 0.15 \pm 0.01$, while in toluene solution, the quadrupole coupling constant has been reported as 0.49 MHz.[21] These data clearly demonstrate the marked dependence of C_Q on solvation. The EFG tensor components depend inversely on the cube of the distance between the nucleus of interest and the individual surrounding electrons; the value of $\langle 1/r^3 \rangle$ is still significant even many angstroms away from the nucleus.

The most sensitive parameter in fitting the spectra of MAS samples was the difference in isotropic chemical shifts for the two sites, $\Delta\delta_{iso}$. In particular, the spectrum obtained at 9.4 T was very sensitive to this parameter; adjusting $\Delta\delta_{iso}$ by as little as 0.01 ppm was noticeable in the simulated line shape. The best-fit chemical shift tensor components for each of the sites and $\Delta\delta_{iso}$ are also given in Table 1. The second-order quadrupolar shift for each of the two sites were calculated using eq 11.[31] For site 1, the second-order quadrupolar shift was determined to be $\Delta\nu_{+1/2,-1/2} = 39$ Hz, while for site 2 the shift was found to be 40 Hz. For beryllium, these displacements are significant; at 9.4 T they represent about 2% of the total known chemical shift range. By use of expressions derived by Samoson,[31] it was also possible to calculate the theoretical positions of the satellite transition centerbands with respect to the central transition centerband (eq 12). The satellite transition centerband maxima are clearly apparent in Figure 2 (indicated by asterisks), owing to a favorable C_Q^2/ν_L ratio. The calculated displacement of 119 Hz at 9.4 T is in excellent agreement with the observed shift. Shown in Figure 3 are the central transitions of the experimental and simulated spectra of MAS samples acquired with $B_0 = 4.7$ T. The necessity of obtaining spectra at two different applied magnetic fields is apparent here. Since the chemical shift difference of 0.22 ppm is reduced by a factor of 2 (in Hz) at this lower field, its effect is essentially negligible, and thus, this spectrum at 4.7 T could be fit reasonably on the basis of a single-site model. The satellite transition centerbands are displaced from the central transition centerbands by 238 Hz at 4.7 T; their intensities are too weak to be apparent in Figure 3.

After having established the quadrupolar parameters for each of the sites, the possibility of anisotropic beryllium chemical shielding was investigated by acquiring spectra of stationary samples at 4.7 and 9.4 T. In Figure 4, it is clearly evident that the spans of the beryllium shielding tensors are nonzero. For a stationary sample with $B_0 = 9.4$ T, the experimental and calculated ^{9}Be NMR spectra are presented. The lower trace is the calculated spectrum for the case where $\Omega = 0$ ppm for both beryllium sites. Above this is a calculated spectrum that matches

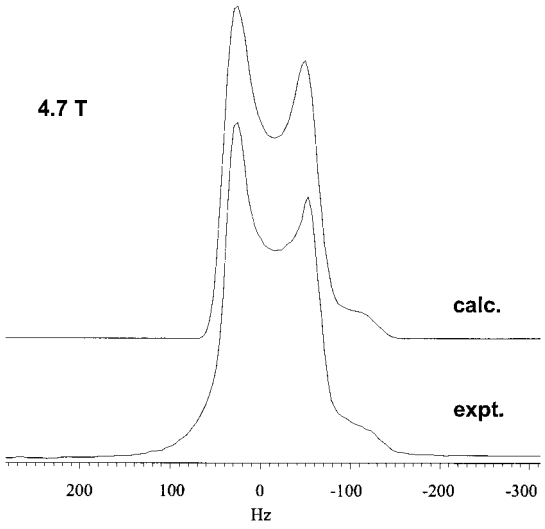

Figure 3. Experimental and calculated ^{9}Be NMR spectra of a MAS sample of solid Be(acac)$_2$, with $\nu_{rot} = 5.0$ kHz, $B_0 = 4.7$ T, and $\nu_L = 28.1$ MHz. The experimental spectrum is the sum of 1024 acquisitions. Best-fit simulation parameters are given in Table 1.

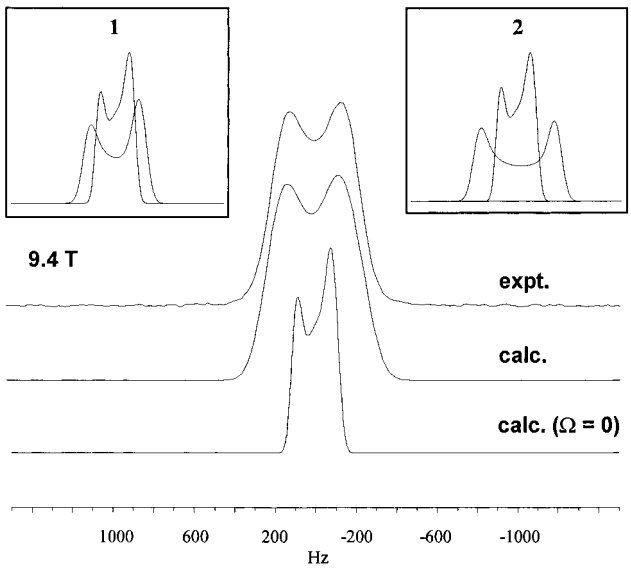

Figure 4. Experimental and calculated ^{9}Be NMR spectra of a stationary sample of solid Be(acac)$_2$, with $B_0 = 9.4$ T and $\nu_L = 56.2$ MHz. The experimental spectrum is the sum of 1536 acquisitions. The lower trace shows the simulated spectrum when a span of zero is assumed, and the middle trace is the simulated spectrum when the best-fit parameters given in Table 1 are used. Shown in the insets are simulations for each of the two sites; the narrow traces correspond to a span of zero, and the wider traces correspond to the best-fit spans.

the experimental spectrum; the spans are nonzero. The span of the chemical shift tensor for site 1 was determined to be 3.42 ppm, while the corresponding span for site 2 was found to be 6.60 ppm. Shown in Table 1 are the chemical shift parameters used to generate the best-fit spectrum. On the basis of the formal D_{2d} symmetry of an isolated Be(acac)$_2$ molecule, the assumption was made that the shielding tensors were axially symmetric, with the unique component for each site along the unique C_2 axis in each site (Figure 1). The Euler angles α, β, and γ describe the rotations required to bring the principal axis system (PAS) of the EFG tensor into coincidence with the PAS of the CS tensor.[41] Thus, by setting all angles to zero, we make the assumption that the CS and EFG tensors are exactly coincident. This is a reasonable assumption, since it is expected that the principal axis systems of both the CS and EFG tensors will be

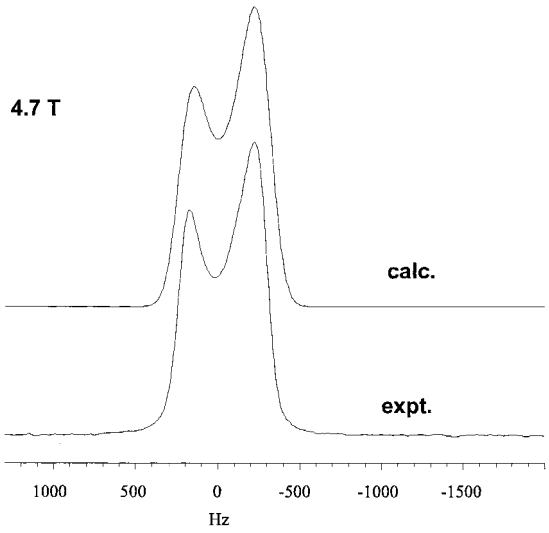

Figure 5. Experimental and calculated ^{9}Be NMR spectra of a stationary sample of solid Be(acac)$_2$, with $B_0 = 4.7$ T and $\nu_L = 28.1$ MHz. The experimental spectrum is the sum of 1536 acquisitions. Best-fit simulation parameters are given in Table 1.

TABLE 2: Best-Fit ^{9}Be Chemical Shift Parameters for Noncoincident CS and EFG Tensors in Be(acac)$_2$

	site 1	site 2
δ_{11}/ppm	3.00	2.00
δ_{22}/ppm	3.00	1.50
δ_{33}/ppm	−3.84	−2.00
Ω/ppm	6.84	4.00
α [a]/deg	0	0
β/deg	14	14
γ/deg	0	0

[a] Euler angles describe the rotations required to bring the EFG tensor into coincidence with the CS tensor.

approximately coincident with the three C_2 axes shown in Figure 1. This supposition is supported by ab initio calculations (vide infra). Shown in the insets of Figure 4 are central transition centerband simulations for each of the two sites. The narrower line shapes correspond to a span of zero, and the wider line shapes represent the best fits, where Ω is nonzero. From these simulations and comparison with the experimental spectrum, it is clear that shielding anisotropy plays a significant role in determining the overall line shape for the static samples. The spectrum obtained at 4.7 T confirms this conclusion (Figure 5); an excellent fit is obtained using identical simulation parameters (Table 1). It should be pointed out, however, that owing to the narrow breadth of the spectra of stationary samples and owing to the small shielding range of beryllium, other chemical shift parameters could be employed to fit these spectra. For example, excellent fits at both fields were obtained by using the parameters shown in Table 2. For this set of parameters, the Euler angle β for both sites was set to 14°; this implies that the EFG and CS tensors are not coincident. However, in this case, nonaxial symmetry of the shielding tensor was required for a good fit. It is possible that other CS parameters would also give acceptable fits to the experimental spectra. Thus, although we cannot definitively conclude that the chemical shift parameters given in Table 1 are the most appropriate, consideration of the data in Tables 1 and 2, as well as further attempts at simulating the spectra, allows us to establish upper and lower limits on Ω(^{9}Be) in Be(acac)$_2$ of 7 and 3 ppm.

Ab Initio Calculations. *(i) Be(acac)$_2$.* Ab initio calculations were performed to determine magnitudes and orientations of the CS and EFG tensors for comparison with the conclusions reached experimentally. Eigenvalues and direction cosines relating the tensors to the molecular frame were determined by diagonalization of the symmetrized tensors. Table 3 summarizes the results of the calculations for Be(acac)$_2$, based on atomic coordinates from both the crystal structure and the gas-phase electron diffraction data. Calculations were done using three different geometries: molecule 1, molecule 2 (after ref 24), and the gas-phase electron diffraction data.[23] Distances of 1.09 Å were used for C−H bonds. Both unique molecules in the crystal structure have the Be atom chelated in a distorted tetrahedron, with intrachelate O−Be−O bond angles of 107.5°.[24] For molecule 1, each of the acetylacetonato rings are approximately planar, and the angle between one of the methine carbons, the beryllium atom, and the other methine carbon is 178° (see Figures 1 and 6A). Thus, these molecules possess near-D_{2d} symmetry. Molecule 2, however, is relatively distorted. Its chelate rings are somewhat twisted, and the angle described above is 165° (see Figure 6A). Such distortions should affect the orientation of the CS and EFG tensors in the molecular frame. In the electron diffraction study,[23] D_{2d} symmetry was imposed on the molecule in order to solve the structure. Thus, calculations based on these coordinates should place the principal axes of the CS and EFG tensors along the three symmetry axes (Figure 1).

For molecules 1 and 2, calculations were done at the RHF level using the 6-311+G* basis set on all atoms, and again with the larger 6-311++G(3df,3pd) basis set substituted on the beryllium and oxygen atoms. As shown in Table 3, the calculated shielding tensor is approximately axially symmetric in all cases, with spans ranging from 7.0 to 9.0 ppm. The calculated spans are in agreement with the upper experimentally determined limit of 7 ppm. Although these spans are quite small in the context of the shielding anisotropies of more commonly studied nuclei (^{13}C, ^{31}P, etc.), they are nevertheless nonzero according to both theory and experiment. In fact, a span of 7 ppm represents a considerable fraction of the total known shift range for ^{9}Be of less than 50 ppm. The isotropic values of the shielding tensor are 0.6 ppm apart for molecules 1 and 2, in reasonable agreement with the experimentally determined $\Delta\delta_{iso}$ value of 0.22 ± 0.01 ppm. The effect of the locally dense basis set on the CS tensor results is minimal; a slightly more substantial effect is noted for C_Q and η. In addition to providing numerical values for the quadrupolar coupling constant, ab initio calculations also indicate the sign of this quantity; in the case of Be in Be(acac)$_2$ the sign is negative.[42] At the RHF/6-311+G* level, the results are already in very good quantitative agreement with experimental results. Applying a locally dense basis set to Be and O (RHF/6-311++G(3df,3pd)) improves the agreement; both the experimental and calculated $|C_Q|$s are on the order of 300 kHz. Also of interest in the results of the higher-level calculations is the improvement of the η values. The use of the larger basis set results in a reduction of the asymmetry parameter toward the experimental value; however, there is still not quantitative agreement. In general, one of the difficulties associated with the calculation of EFG tensors is the poor description of the electron distribution in the vicinity of the nucleus provided by Gaussian-type orbitals. Calculations done using the gas-phase electron-diffraction data yielded axially symmetric CS and EFG tensors, as shown in Table 3. The isotropic value as well as the span of the shielding tensor are both very similar to the results based on the X-ray crystal structure data. The quadrupolar coupling constant of −306 kHz is in excellent agreement with experimental results, although this must be fortuitous given the fact that the calculations were

TABLE 3: Results of Ab Initio Calculations of the Beryllium CS and EFG Tensors of Be(acac)$_2$

input coordinates	computational level	σ_{11}/ppm	σ_{22}/ppm	σ_{33}/ppm	σ_{iso}/ppm	Ω/ppm	C_Q/kHz	η
crystal structure,[a] molecule 1	RHF/6-311+G*	110.4	110.9	117.4	112.9	7.0	−182	0.30
crystal structure,[a] molecule 2	RHF/6-311+G*	110.2	111.2	119.1	113.5	8.9	−275	0.39
crystal structure,[a] molecule 1	RHF/6-311++G(3df,3pd) on Be and O;	108.8	109.3	116.1	111.4	7.3	−241	0.24
crystal structure,[a] molecule 2	6-311+G* on remaining atoms	108.7	109.6	117.7	112.0	9.0	−309	0.26
electron diffraction data[b]	RHF/6-311++G(3df,3pd) on Be and O; 6-311+G* on remaining atoms	108.7	108.7	115.7	111.0	7.0	−306	0

[a] Reference 24. C−H bond lengths were set to 1.09 Å. [b] Reference 23. C−H bond lengths were set to 1.09 Å.

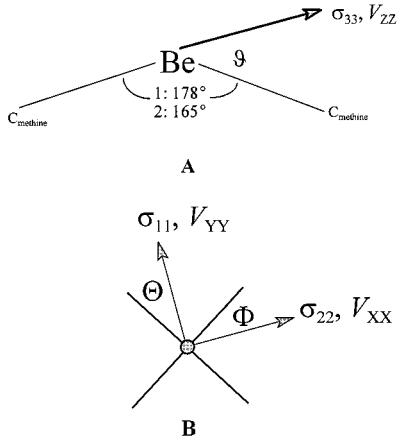

Figure 6. Definition of the angles Θ, Φ, and ϑ, which are used to define the ^{9}Be CS and EFG tensor orientations with respect to the Be(acac)$_2$ molecular frame. The angle ϑ, shown in part A, is the angle between the largest component of the tensor and the nearest Be−C(methine) vector. For molecule 1, the angle between one C(methine), the central Be atom, and the other C(methine) is 178°; for molecule 2 this angle is 165°. Shown in part B is a view along the Be−C(methine) vector used to define ϑ. The Be atom is at the center and is coordinated approximately tetrahedrally by four oxygen atoms (see Figure 1B). In this projection, Θ is the angle between σ_{11} (or V_{YY}) and the nearest Be−O bond and Φ is the angle between σ_{22} (or V_{XX}) and the nearest Be−O bond. See the text for more discussion, and see Table 4 for a summary of the results.

done on isolated molecules and the experiments were done in the solid state, where intermolecular interactions surely influence the CS and EFG tensors. In any case, it would appear in this case that contributions from the lattice are small. This is also supported by the good agreement between the solution and solid-state values.

As alluded to earlier, ab initio calculations also provide an indication of the orientation of the CS and EFG tensors in their PASs with respect to the molecular frame. To describe the orientations, it is convenient to use the three angles indicated in Figure 6 (ϑ, Θ, and Φ) and the data of Table 4. The angle ϑ is that between the direction of the largest component of the tensor and the nearest Be−C(methine) internuclear vector (Figure 6A). Figure 6B is a view along the vector connecting the C(methine) to the central Be, with the Be atom at the center and the four oxygen atoms arranged approximately tetrahedrally around this; the angles between the Be−O bonds are approximately 90°. The angle between σ_{11} (or V_{YY} in the case of the EFG tensor) and the nearest Be−O bond is denoted by Θ. The angle between the remaining component (σ_{22} or V_{XX}) and the nearest Be−O bond is denoted by Φ. For perfect D_{2d} symmetry, one would expect $\Theta = \Phi = 45°$; $\vartheta = 0$. The results based on the crystal structure show significant deviations from this ideal case; they are summarized in Table 4. The data demonstrate that even in an environment of fairly high symmetry, the CS and EFG tensors are not exactly coincident. In fact, although the unique components both lie near the direction of the approximate unique C_2 axis, the remaining two components are reversed for the two tensors (σ_{11} is nearly coincident with V_{YY}, not V_{XX}); this is not surprising in the present case of near-axial symmetry. A calculation carried out using the atomic coordinates from electron diffraction data confirms the expectation that the principal axes of the CS and EFG tensors lie along the three perpendicular C_2 axes when the environment around Be is highly symmetric.

On the basis of the known distorted geometry of molecule 2,[24] we can conclude that site 2 from the analysis of the NMR spectra likely corresponds to molecule 2 and that site 1 corresponds to molecule 1. This is evident when we compare the experimental and calculated results for C_Q, η, and Ω. Experimentally, site 1 has the smaller span, the smaller C_Q value, and the smaller η value (Table 1); the calculations reproduce these findings.

(ii) Other Beryllium Compounds. To put the shielding results obtained for Be(acac)$_2$ in context, we have carried out calculations on a series of beryllium-containing compounds that are known to be representative of the chemical shift range for ^{9}Be in solution.[11] Table 5 summarizes the results, including the tensor components. Shown in Figure 7 is a plot of the isotropic shielding constants, with dimethylberyllium being the most deshielded at 84.1 ppm and cyclopentadienyl beryllium borohydride being the most shielded at 137.3 ppm. For comparison, the known chemical shift values in solution are included in Table 5. The calculations perform well over the entire range of known beryllium chemical shifts. For example, the isotropic chemical shift of $C_5H_5BeBH_4$ with respect to $Be(H_2O)_4^{2+}$ as determined by ab initio calculations is −22.3 ppm; the experimental value for $C_5H_5BeBH_4$ in hexafluorobenzene is −22.1 ppm. At the other extreme of known beryllium chemical shifts are a series of three-coordinate compounds recently prepared by Niemeyer and Power.[44] The three-coordinate beryllium compound, ArBeSMes*(OEt$_2$) (Ar = $-C_6H_3$-2,6-Mes$_2$; Mes = $-C_6H_2$-2,4,6-Me$_3$; Mes* = $-C_6H_2$-2,4,6-*t*-Bu$_3$), has a chemical shift of 17.4 ppm in deuterated benzene at 20 °C; calculations on a smaller model three-coordinate compound $CH_3BeSH(OMe_2)$ indicate a value of 18.4 ppm. Atomic coordinates from the crystal structure data for ArBeSMes*(OEt$_2$) were used to set up the calculation on the model compound; experimental bond lengths and angles were kept intact. It is important to emphasize that all of the calculations were carried out on isolated molecules and that outer-sphere solvation will in general have an effect on the experimentally observed chemical shifts. Despite this,

TABLE 4: Orientations of the ^{9}Be CS and EFG Tensors in $Be(acac)_2$ with Respect to the Molecular Frame[a]

structure	computational level	interaction tensor	Θ/deg	Φ/deg	ϑ/deg
molecule 1	RHF/6-311+G*	CS	12	12°	1
		EFG	14	14	1
molecule 1	RHF/6-311++G(3df,3pd)[b]	CS	13	12	1
		EFG	15	14	2
molecule 2	RHF/6-311+G*	CS	12	18	21
		EFG	1	11	37
molecule 2	RHF/6-311++G(3df,3pd)[b]	CS	14	20	21
		EFG	2	7	32
electron diffraction data	RHF/6-311++G(3df,3pd)[b]	CS	45	45	0
		EFG	45	45	0

[a] See the text and Figure 6 for definitions and interpretation of the angles. [b] 6-311++G(3df,3pd) on Be and O atoms; 6-311+G* on remaining atoms.

TABLE 5: Calculated ^{9}Be Nuclear Magnetic Shielding Tensor Components for a Representative Series of Beryllium-Containing Compounds (RHF/6-311++G(3df,3pd))[p]

compound	σ_{11}/ppm	σ_{22}/ppm	σ_{33}/ppm	σ_{iso}/ppm	δ_{iso}/ppm (calc)	δ_{iso}/ppm (expt)
$Be(CH_3)_2$[a]	46.9	47.7	157.6	84.1	30.9	
$H_3C-Be-H$[b]	50.4	50.4	153.4	84.7	30.3	
BeH_2[b]	57.0	57.0	148.9	87.7	27.3	
three-coordinate[c]	84.2	88.5	117.0	96.6	18.4	17.4[d]
$BeBr_2$[b]	60.7	60.7	170.8	97.4	17.6	
Cl−Be−H[b]	67.9	67.9	158.1	97.9	17.1	
$BeCl_2$[e]	68.6	68.6	167.0	101.4	13.6	
Be_2Cl_4[f]	88.3	89.4	131.9	103.2	11.8	
F−Be−H[b]	83.4	83.4	156.3	107.7	7.3	
$Be(acac)_2$	108.8	109.5	116.9	111.7	3.3	0.50, 0.72[g]
BeF_2[b]	86.9	86.9	162.7	112.1	2.9	
$Be(H_2O)_4^{2+}$ [h]	114.1	115.1	115.7	115.0	0.0	0.0
BeF_4^{2-} [i]	115.9	115.9	115.9	115.9	−0.9	∼ −2[j]
C_5H_5BeCl[k]	110.7	110.7	180.0	133.8	−18.8	−19.1[l]
$C_5H_5BeCH_3$[m]	118.6	118.6	174.1	137.1	−22.1	−20.4[n]
$C_5H_5BeBH_4$[o]	117.2	120.4	174.2	137.3	−22.3	−22.1[l]

[a] An equilibrium Be−C bond length of 1.698 Å was used;[43] C−H bond lengths of 1.09 Å were used. [b] The geometry was optimized at the RHF/6-311++G(3df,3pd) level. [c] The calculation was done on a model three-coordinate beryllium compound, while the reported experimental chemical shift is for a larger compound. See text for details. [d] In benzene. From ref 44. See text for structure of compound. [e] An equilibrium Be−Cl bond length of 1.80 Å was used.[45] [f] Geometry from ref 45. [g] This work (solid state). Values are the average for the two unique molecules in the crystal structure (see Table 3). Referenced with respect to $BeSO_4$(aq) as $Be(H_2O)_4^{2+}$. [h] A Be−O bond length of 1.610 Å was used.[46] [i] A Be−F bond length of 1.53 Å was used.[47]. [j] As the ammonium salt in water. From ref 48. [k] Geometry from ref 49. C−H bond lengths were set to 1.09 Å. [l] In hexafluorobenzene. From ref 11a. [m] Geometry from ref 50. C−H bond lengths were set to 1.09 Å. [n] In pentane/CF_3Br. From ref 11a. [o] Geometry from refs 51 and 52. C−H bond lengths were set to 1.09 Å. [p] Isotropic chemical shifts are referenced with respect to $Be(NO_3)_2$ (aq) as $Be(H_2O)_4^{2+}$ unless otherwise indicated.

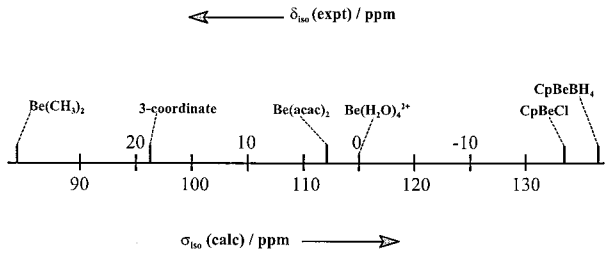

Figure 7. Beryllium-9 isotropic chemical shielding constants (σ_{iso}) and isotropic chemical shifts (δ_{iso}), based on ab initio calculations of the chemical shielding tensors. See Table 5 for a complete listing of the data.

the agreement between δ_{iso}(calc) and δ_{iso}(expt) is superb for the range of compounds investigated.

Several linear molecules were also examined. The nuclear magnetic shielding tensors of linear molecules are of particular interest because of the fact that the paramagnetic component of the shielding is zero along the C_∞ axis.[53] Therefore, the σ_{33} component, which lies along this axis, will be approximately equal to the free-atom value of the diamagnetic portion, which has been calculated as 149.26 [54] and 152.7 ppm.[55] For the linear molecules examined in the present study, BeH_2, $BeBr_2$, ClBeH, $BeCl_2$, FBeH, and BeF_2, the most shielded component was found to range from 148.9 to 170.8 ppm (see Table 5). The pseudo-linear molecules $Be(CH_3)_2$ and H_3CBeH also have their most shielded components within this range. It is obvious from the data shown for the linear molecules in Table 5 that the paramagnetic contribution to shielding in beryllium is significant. For example, the perpendicular shielding component in BeH_2 is 57.0 ppm; this represents a paramagnetic contribution of about −92 ppm. These results disprove the assumption that the chemical shift of beryllium is governed essentially by the diamagnetic term.[27,28]

Of the halogens Cl, Br, and I, chlorine as a substituent generally leads to the least shielding of nucleus E in compounds of the type EXH_3 (e.g., E = C, Si), while X = I leads to the greatest shielding of E. This is quite general and is designated the normal halogen dependence (NHD);[56] however, exceptions are known—notably for early transition metals in their highest oxidation states.[57] In the case of beryllium compounds of the type BeX_2 (X = F, Cl, Br), the ab initio calculations predict that beryllium is least shielded for X = Br and most shielded for X = F; this is a case of the inverse halogen dependence (IHD). A similar trend has been predicted for the group 13 nuclei

in BX, AlX, and GaX; variations in the HOMO−LUMO gap are responsible for this trend.[58]

There is no established absolute experimental shielding scale for ^{9}Be at present. A literature search did not reveal any experimentally determined spin−rotation constants from which a scale could be established. In the absence of spin−rotation data, high-level calculations on $Be(H_2O)_4^{2+}$ serve as a starting point for converting experimental chemical shift tensors to shielding tensors. Because of its very small size and resulting high charge density, the Be^{2+} ion is solvated by four water molecules in aqueous solution (rather than six); the Be−O bonds are highly covalent compared to other aqua ions.[59,60] This results in a large difference in the isotropic shielding constants of Be^{2+} and $Be(H_2O)_4^{2+}$. Our calculated value of $\sigma_{iso} = 114.96$ ppm (RHF/6-311++G(3df,3pd)) for the tetrahydrate cation is similar to the results obtained recently by Tossell:[61] 115.33 ppm (RHF/6-311G(2d,p) and 112.66 ppm (BLYP/6-31G*). For comparison, Feiock and Johnson[55] report a relativistic isotropic shielding constant for the isolated Be^{2+} cation of 131.2 ppm, and Saxena and Narasimhan[62] give a similar value, $\sigma_{iso} = 130.9$ ppm, which was obtained using Hartree−Fock−Slater wave functions.

The spans of the shielding tensors for many of the molecules examined are much greater than the total known shielding range of ~50 ppm (see Table 5). For instance, the span of the ^{9}Be CS tensor in dimethylberyllium is over 110 ppm, and in the cyclopentadienyl complexes the spans are all in excess of 50 ppm. More interesting is the case of the BeH^- anion. This ion is particularly challenging for computational methods because of its very small HOMO−LUMO gap (0.080 au) and its very loosely bound outer electrons.[63] Diffuse functions and proper treatment of electron correlation are essential for accurate calculations on this ion.[63,64] Our RHF/6-311++G(3df,3pd) calculation of the beryllium CS tensor in BeH^- produced a span of nearly 200 ppm. While we cannot claim absolute accuracy of this result owing to the difficulties described above, this span is extraordinarily large for beryllium. Calculations on BeH_2, another compound with only formally s electrons, yielded a CS tensor with a span of more than 90 ppm.

Conclusions

The present combined solid-state NMR and ab initio investigation of $Be(acac)_2$ has shown, for the first time, a definite anisotropy in the chemical shielding tensor of beryllium. Through the analyses of spectra of stationary and MAS samples, upper and lower limits on the span of the beryllium shielding tensor were found to be 7 and 3 ppm. Ab initio calculations of the electric field gradient and chemical shielding tensors compare well with the experimental results, placing upper and lower limits of 9.0 and 7.0 ppm on Ω. The calculations also indicate the effects of deviation from perfect point group symmetry on the CS and EFG tensor orientations. The principal axes of the NMR interaction tensors of the Be nucleus in a $Be(acac)_2$ molecule of perfect D_{2d} symmetry are coincident with the three C_2 axes of this point group. However, in the two unique, distorted molecules in the unit cell, the alignments of the principal axis systems become quite sensitive to the local geometry, and the CS and EFG tensor principal axis systems are no longer exactly coincident. The results of further calculations of CS tensors on a series of beryllium-containing compounds compare very well with the isotropic chemical shifts, which are known experimentally. The paramagnetic part of the shielding tensor has been proven to play a significant role in determining the overall isotropic Be shielding constants, as evidenced by calculations on a series of linear molecules. The accurate experimental measurement of a ^{9}Be spin−rotation constant for a molecule that one can also investigate via conventional NMR techniques is a prerequisite for the establishment of a reliable absolute ^{9}Be shielding scale.

Acknowledgment. The authors thank the members of the solid-state NMR group at Dalhousie University for many helpful comments. Professor G. H. Penner is thanked for providing the sample of $Be(acac)_2$. Professor T. S. Cameron is acknowledged for carrying out crystallographic database searches for some of the beryllium compounds studied herein. R.E.W. is grateful to NSERC (Canada) for a major installation grant to purchase a new console for our 4.7 T magnet and for a research (operating) grant. D.L.B. is grateful to NSERC and to the Izaak Walton Killam Trust for postgraduate scholarships. All spectra were obtained at the Atlantic Region Magnetic Resonance Centre, which is also supported by NSERC.

References and Notes

(1) Jäger, C. In *NMR Basic Principles and Progress*; Diehl, P., Fluck, E., Günther, H., Kosfeld, R., Seelig, J., Eds.; Springer-Verlag: Berlin, 1994; Vol. 31, pp 133−170.

(2) Freude, D.; Haase, J. In *NMR Basic Principles and Progress*; Diehl, P., Fluck, E., Günther, H., Kosfeld, R., Seelig, J., Eds.; Springer-Verlag: Berlin, 1993; Vol. 29, pp 1−90.

(3) Smith, M. E.; Strange, J. H. *Meas. Sci. Technol.* **1996**, *7*, 449.

(4) Jarvie, T. P.; Mueller, K. T. *Adv. Anal. Geochem.* **1995**, *2*, 141.

(5) Smith, M. E.; van Eck, E. R. H. *Prog. Nucl. Magn. Reson. Spectrosc.* **1999**, *34*, 159.

(6) *Modeling NMR Chemical Shifts: Gaining Insights into Structure and Environment*; Facelli, J. C., de Dios, A. C., Eds.; ACS Symposium Series 732; ACS Books: Washington, DC, 1999.

(7) Jameson, C. J.; de Dios, A. C. In *Nuclear Magnetic Resonance: A Specialist Periodical Report*; Webb, G. A., Ed.; Royal Society of Chemistry: Cambridge, 1999; Vol. 28, Chapter 2. See also previous volumes in this series.

(8) Helgaker, T.; Jaszuński, M.; Ruud, K. *Chem. Rev.* **1999**, *99*, 293.

(9) (a) Sundholm, D.; Olsen, J. *Chem. Phys. Lett.* **1991**, *177*, 91. (b) Pyykkö, P. *Z. Naturforsch.* **1992**, *47a*, 189.

(10) *Gmelin Handbook of Inorganic Chemistry*, 8th ed.; (prepared by the Gmelin-Institut für Anorganische Chemie der Max-Planck-Gesellschaft zur Förderung der Wissenschaften); Springer-Verlag: Berlin, 1986; Vol. A1, Section 8.

(11) (a) Gaines, D. F.; Coleson, K. M.; Hillenbrand, D. F. *J. Magn. Reson.* **1981**, *44*, 84. (b) Akitt, J. W. In *Multinuclear NMR*; Mason, J., Ed.; Plenum Press: New York, 1987; Chapter 7.

(12) (a) Sherriff, B. L.; Grundy, H. D.; Hartman, J. S.; Hawthorne, F. C.; Černý, P. *Can. Mineral.* **1991**, *29*, 271. (b) Nenoff, T. M.; Harrison, W. T. A.; Gier, T. E.; Nicol, J. M.; Stucky, G. D. *Zeolites* **1992**, *12*, 770. (c) Harrison, W. T. A.; Nenoff, T. M.; Gier, T. E.; Stucky, G. D. *Inorg. Chem.* **1993**, *32*, 2437. (d) Ahrens, E. T.; Hammel, P. C.; Heffner, R. H.; Reyes, A. P.; Smith, J. L.; Clark, W. G. *Phys. Rev. B* **1993**, *48*, 6691. (e) Han, S.; Schmitt, K. D.; Shihabi, D. S.; Chang, C. D. *J. Chem. Soc., Chem. Commun.* **1993**, 1287. (f) Xu, Z.; Sherriff, B. L. *Can. Mineral.* **1994**, *32*, 935. (g) Harrison, W. T. A.; Nenoff, T. M.; Gier, T. E.; Stucky, G. D. *J. Solid State Chem.* **1994**, *111*, 224. (h) Yeom, T. H.; Lim, A. R.; Choh, S. H.; Hong, K. S.; Yu, Y. M. *J. Phys.: Condens. Matter* **1995**, *7*, 6117. (i) Dann, S. E.; Weller, M. T. *Sol. State Nucl. Magn. Reson.* **1997**, *10*, 89. (j) Tang, X.-P.; Busch, R.; Johnson, W. L.; Wu, Y. *Phys. Rev. Lett.* **1998**, *81*, 5358.

(13) Everest, D. A. In *Comprehensive Inorganic Chemistry*; Bailar, J. C., Emeléus, H. J., Nyholm, R., Trotman-Dickenson, A. F., Eds.; Pergamon Press: Oxford, 1973; Chapter 9.

(14) Wehrli, F. W. *J. Magn. Reson.* **1978**, *30*, 193.

(15) Kanakubo, M.; Ikeuchi, H.; Satô, G. P. *J. Chem. Soc., Faraday Trans.* **1998**, *94*, 3237.

(16) Kanakubo, M.; Ikeuchi, H.; Satô, G. P. *J. Mol. Liq.* **1995**, *65/66*, 273.

(17) Kanakubo, M.; Ikeuchi, H.; Satô, G. P. *J. Magn. Reson.* **1995**, *112A*, 13.

(18) Eichele, K.; Chan, J. C. C.; Wasylishen, R. E.; Britten, J. F. *J. Phys. Chem. A* **1997**, *101*, 5423.

(19) Schurko, R. W.; Wasylishen, R. E.; Foerster, H. *J. Phys. Chem. A* **1998**, *102*, 9750.

(20) Barrie, P. J. *Chem. Phys. Lett.* **1993**, *208*, 486.

(21) Dechter, J. J.; Henriksson, U.; Kowalewski, J.; Nilsson, A.-C. *J. Magn. Reson.* **1982**, *48*, 503.

(22) Kowalewski, J.; Maliniak, A. *J. Magn. Reson.* **1985**, *62*, 316.
(23) Shibata, S.; Ohta, M.; Iijima, K. *J. Mol. Struct.* **1980,** *67*, 245.
(24) Onuma, S.; Shibata, S. *Acta Crystallogr.* **1985**, *C41*, 1181.
(25) Wehrli, F. W.; Wehrli, S. L. *J. Magn. Reson.* **1982**, *47*, 151.
(26) (a) Haeberlen, U. In *Advances in Magnetic Resonance*; Waugh, J. S., Ed.; Academic Press: New York, 1976; Supplement 1, Chapter VI. (b) Duncan, T. M. *Principal Components of Chemical Shift Tensors: A Compilation*, 2nd ed.; Farragut Press: Chicago, 1994.
(27) Kovar, R. A.; Morgan, G. L. *J. Am. Chem. Soc.* **1970**, *92*, 5067.
(28) Granger, P. In *NMR of Newly Accessible Nuclei*; Laszlo, P., Ed.; Academic Press: New York, 1983; Vol. 2, pp 386−387.
(29) Mason, J. *Solid State Nucl. Magn. Reson.* **1993**, *2*, 285.
(30) Taulelle, F. In *Multinuclear Magnetic Resonance in Liquids and Solids−Chemical Applications*; Granger, P., Harris, R. K., Eds.; Kluwer Academic Publishers: Dordrecht, 1990; pp 393−407.
(31) Samoson, A. *Chem. Phys. Lett.* **1985**, *119*, 29.
(32) Eichele, K.; Wasylishen, R. E. WSOLIDS1 NMR Simulation Package, version 1.17.21, 1998.
(33) Alderman, D. W.; Solum, M. S.; Grant, D. M. *J. Chem. Phys.* **1986**, *84*, 3717.
(34) Frisch, M. J.; Trucks, G. W.; Schlegel, H. B.; Gill, P. M. W.; Johnson, B. G.; Robb, M. A.; Cheeseman, J. R.; Keith, T.; Petersson, G. A.; Montgomery, J. A.; Raghavachari, K.; Al-Laham, M. A.; Zakrzewski, V. G.; Ortiz, J. V.; Foresman, J. B.; Peng, C. Y.; Ayala, P. Y.; Chen, W.; Wong, M. W.; Andres, J. L.; Replogle, E. S.; Gomperts, R.; Martin, R. L.; Fox, D. J.; Binkley, J. S.; Defrees, D. J.; Baker, J.; Stewart, J. P.; Head-Gordon, M.; Gonzalez, C.; Pople, J. A. *Gaussian 94*, revision B.3; Gaussian, Inc.: Pittsburgh, PA, 1995.
(35) Frisch, M. J.; Trucks, G. W.; Schlegel, H. B.; Scuseria, G. E.; Robb, M. A.; Cheeseman, J. R.; Zakrzewski, V. G.; Montgomery, J. A.; Stratmann, R. E.; Burant, J. C.; Dapprich, S.; Millam, J. M.; Daniels, A. D.; Kudin, K. N.; Strain, M. C.; Farkas, O.; Tomasi, J.; Barone, V.; Cossi, M.; Cammi, R.; Mennucci, B.; Pomelli, C.; Adamo, C.; Clifford, S.; Ochterski, J.; Petersson, G. A.; Ayala, P. Y.; Cui, Q.; Morokuma, K.; Malick, D. K.; Rabuck, A. D.; Raghavachari, K.; Foresman, J. B.; Cioslowski, J.; Ortiz, J. V.; Stefanov, B. B.; Liu, G.; Liashenko, A.; Piskorz, P.; Komaromi, I.; Gomperts, R.; Martin, R. L.; Fox, D. J.; Keith, T.; Al-Laham, M. A.; Peng, C. Y.; Nanayakkara, A.; Gonzalez, C.; Challacombe, M.; Gill, P. M. W.; Johnson, B. G.; Chen, W.; Wong, M. W.; Andres, J. L.; Head-Gordon, M.; Replogle, E. S.; Pople, J. A. *Gaussian 98*, revision A.2; Gaussian, Inc.: Pittsburgh, PA, 1998.
(36) Basis sets were obtained from the Extensible Computational Chemistry Environment Basis Set Database, version 1.0, as developed and distributed by the Molecular Science Computing Facility, Environmental and Molecular Sciences Laboratory, which is part of the Pacific Northwest Laboratory, P.O. Box 999, Richland, WA 99352, and funded by the U.S. Department of Energy. The Pacific Northwest Laboratory is a multiprogram laboratory operated by Battelle Memorial Institute for the U.S. Department of Energy under Contract DE-AC06-76RLO 1830. Contact David Feller or Karen Schuchardt for further information.
(37) Ditchfield, R. *Mol. Phys.* **1974**, *27*, 789.
(38) Wolinski, K.; Hinton, J. F.; Pulay, P. *J. Am. Chem. Soc.* **1990**, *112*, 8251.
(39) Skibsted, J.; Nielsen, N. C.; Bildsøe, H.; Jakobsen, H. J. *J. Magn. Reson.* **1991**, *95*, 88.
(40) Busse, S. C. Ph.D. Thesis, Montana State University, 1986.
(41) For a discussion of Euler angles, see, for example: Schmidt-Rohr, K.; Spiess, H. W. *Multidimensional Solid-State NMR and Polymers*; Academic Press: London, 1994; Appendix B.
(42) Note that Gaussian 94 and Gaussian 98 give the electric field gradient tensor eigenvalues with a sign convention opposite to that used in eq 9; the Gaussian output has been corrected in the present calculations.
(43) Almenningen, A.; Haaland, A.; Morgan, G. L. *Acta Chem. Scand.* **1969**, *23*, 2921.
(44) Niemeyer, M.; Power, P. P. *Inorg. Chem.* **1997**, *36*, 4688.
(45) Girichev, A. G.; Giricheva, N. I.; Vogt, N.; Girichev, G. V.; Vogt, J. *J. Mol. Struct.* **1996**, *384*, 175.
(46) Dance, I. G.; Freeman, H. C. *Acta Crystallogr.* **1969**, *B25*, 304.
(47) Srivastava, R. C.; Klooster, W. T.; Koetzle, T. F. *Acta Crystallogr.* **1999**, *B55*, 17.
(48) Kotz, J. C.; Schaeffer, R.; Clouse, A. *Inorg. Chem.* **1967**, *6*, 620.
(49) Goddard, R.; Akhtar, J.; Starowieyski, K. B. *J. Organomet. Chem.* **1985**, *282*, 149.
(50) Drew, D. A.; Haaland, A. *Acta Chem. Scand.* **1972**, *26*, 3079.
(51) Drew, D. A.; Gundersen, G.; Haaland, A. *Acta Chem. Scand.* **1972**, *26*, 2147.
(52) Coe, D. A.; Nibler, J. W.; Cook, T. H.; Drew, D.; Morgan, G. L. *J. Chem. Phys.* **1975**, *63*, 4842.
(53) Information on nuclear magnetic shielding tensors in linear molecules and their relationship with the spin−rotation tensor can be found in the following references. (a) Ramsey, N. F. *Molecular Beams*; Oxford University Press: London, 1956. (b) Ramsey, N. F. *Phys. Rev.* **1950**, *78*, 699. (c) Flygare, W. H. *J. Chem. Phys.* **1964**, *41*, 793. (d) Gierke, T. D.; Flygare, W. H. *J. Am. Chem. Soc.* **1972**, *94*, 7277. (e) Flygare, W. H. *Chem. Rev.* **1974**, *74*, 653.
(54) Malli, G.; Froese, C. *Int. J. Quantum Chem.* **1967**, *1S*, 95.
(55) Feiock, F. D.; Johnson, W. R. *Phys. Rev.* **1969**, *187*, 39.
(56) Kidd, R. G. In *Annual Reports on NMR Spectroscopy*; Academic Press: London, 1991; Vol. 23, pp 85−139.
(57) Kaupp, M.; Malkina, O. L.; Malkin, V. G.; Pyykkö, P. *Chem. Eur. J.* **1998**, *4*, 118.
(58) Gee, M.; Wasylishen, R. E. In *Modeling NMR Chemical Shifts: Gaining Insights into Structure and Environment*; Facelli, J. C., de Dios, A. C., Eds.; ACS Symposium Series; American Chemical Society: Washington, DC, 1999.
(59) Richens, D. T. *The Chemistry of Aqua Ions*; John Wiley & Sons: Chichester, 1997; Section 2.3.
(60) Martínez, J. M.; Pappalardo, R. R.; Marcos, E. S. *J. Am. Chem. Soc.* **1999**, *121*, 3175.
(61) Tossell, J. A. *J. Magn. Reson.* **1998**, *135*, 203.
(62) Saxena, K. M. S.; Narasimhan, P. T. *Int. J. Quantum Chem.* **1967**, *1*, 731.
(63) Ruud, K.; Helgaker, T.; Bak, K. L.; Jørgensen, P.; Olsen, J. *Chem. Phys.* **1995**, *195*, 157.
(64) Fowler, P. W.; Steiner, E. *Mol. Phys.* **1991**, *74*, 1147.